Impact of coupling geometry on thermoelectric properties of oligophenyl-base transistor

S Ramezani Akbarabadi, H Rahimpour Soleimani†, M Bagheri Tagani, and Z Golsanamlou

Computational Nanophysics Laboratory (CNL), Department of Physics, University of Guilan, Rasht, P. O. Box 41335-1914, *Iran*

(Received 23 June 2016; revised manuscript received 3 November 2016; published online 10 January 2017)

Thermal and electron transport through organic molecules attached to three-dimensional gold electrodes in two different configurations, namely para and meta with thiol-terminated junctions is studied theoretically in the linear response regime using Green's function formalism. We used thiol-terminated (–SH bond) benzene units and found a positive thermopower because the highest occupied molecular orbital (HOMO) is near the Fermi energy level. We investigated the influence of molecular length and molecular junction geometry on the thermoelectric properties. Our results show that the thermoelectric properties are highly sensitive to the coupling geometry and the molecular length. In addition, we observed that the interference effects and increasing molecular length can increase the thermoelectric efficiency of device in a specific configuration.

Keywords: coupling geometry, figure of merit, Green's function, oligophenyl, thermopower

PACS: 73.50.Lw, 84.60.Bk, 85.80.Fi **DOI:** 10.1088/1674-1056/26/2/027303

1. Introduction

Quantum interference (QI) effects in molecular junctions were recently explored experimentally[1–4] and theoretically.[5–12] For example, a benzene ring coupled to the electrodes in a meta configuration supports low conductance values relative to para-coupled configuration. This observation can be described from the behavior of transmission function of the system. The para configuration has constructive interference (the phase difference between two paths around the ring is zero), whereas the meta configuration has destructive interference.

The thermoelectric effects with improved efficiency, can be thought as an alternative option for the future energy requirements.[13–15] The thermal efficiency of a device is described by a dimensionless quantity as figure of merit, $ZT = S^2 G_e T/\kappa$, which is a function of thermopower or Seebeck coefficient (S), absolute temperature (T), electrical (G_e), and thermal (κ) conductances and $\kappa = \kappa_{el} + \kappa_{ph}$, where κ_{el} is the electron thermal conductance and κ_{ph} denotes the phonon thermal conductance. In recent years, with advent of nanotechnology, it was found that in nanostructures, such as thin films and quantum dots,[16–18] ZT can be increased to 1. In addition to thin films and quantum dots, naowires, nanoribbions, as well as nanotubes have been drawn much attention in studying the thermoelectric properties. Many factors affect on ZT in nanotubes,[19] naowires,[20] and nanoribbions.[21–24] For example, ZT is considerably larger in narrower single-walled carbon nanotubes (SWCNT) because of enhanced Seebeck coefficient. The ZT is decreased by strain as the reduction in the electronic conductance overcomes the reduction in the thermal conductance in SWCNT. The fluctuation of electronic transmissions can strongly enhance thermopower in nanoribbions. Silicon nanowires (SiNWs) oriented along the (111) direction have the largest ZT values while (110) wires have the smallest. This is primarily due to the anisotropic heat conductance in SiNWs.[25] The (110) wires have larger κ_{ph} and thus a smaller ZT. The use of organic molecules are another promising approach.[26–34] In these devices, electrodes Fermi energy can be located too close to the highest occupied orbital (HOMO) or the lowest unoccupied molecular orbital (LUMO), and thus enhancing the thermopower. The thermopower is negative when Fermi energy level is located close to LUMO indicating that the electrons are responsible for transport, and thermopower is positive when Fermi energy level is located close to HOMO denotes the holes are dominant in transport.[29,30] Therefore, thermopower experiment is a tool to identify the kind of carrier responsible in transport mechanism. Thermopower of several molecular junctions attached to Au electrodes has been measured using scanning tunneling microscopy.[15,32,35]

Thermopower measures the voltage gradient ΔV which develops when a small temperature difference is applied under the condition that the net charge current vanishes, $S = -\Delta V/\Delta T|_{I_e=0}$. Theoretical and experimental studies have further analyzed the effect of molecular length,[15,32,35] conformation, and chemical content,[32,36–43] molecular junction geometry,[44–47] anchoring groups,[48–50] and substituents[51] on thermopower. Other studies emphasized the sensitivity of thermopower to fluctuations in molecular structure.[52,53] Experimental measurements of S and conductance were first reported by Ludoph and Ruitenbeek[54] in Au point con-

†Corresponding author. E-mail: rahimpour@guilan.ac.ir

© 2017 Chinese Physical Society and IOP Publishing Ltd

tacts at liquid helium temperatures. Thermopower is experimentally investigated[29,30] for six of the molecules of phenyl-base investigation. The thermopower of several molecular junctions with Au electrodes has been measured using scanning tunneling microscopy.[29,30] Theoretical and experimental studies have further analyzed the effect of molecular length on thermopower.[32,35,41] Ke San-Huang, *et al.*[30] studied the thermoelectric efficiency of a benzene molecular junction coupled to gold electrodes using density functional theory (DFT). They found that increasing the molecular length, leads to an exponential decay of conductance, and considerably enhances S, which ultimately results in an overall decreasing contribution to ZT. Aradhya, *et al.*[35] studied the thermopower of aromatic molecular junction coupled to pyridine- and amine-terminated groups. They found that the amine-terminated molecules conduct through HOMO whereas pyridine-terminated molecules conduct through LUMO, which is in good agreement with theoretical calculations. The same result has been obtained in previous works.[44,45] The difference in value depends on the methods and the accuracy of approximations.

In this paper, we investigate the influence of quantum interference on thermopower property of three organic molecules attached to three-dimensional gold electrodes in two different configurations: para and meta, as depicted in Fig. 1. These selected molecules are phenyl dithiol (PDT), biphenyl dithiol (BPDT), and triphenyl dithiol (TPDT), since they are aromatic organic compounds and have π orbitals that make them an appropriate candidate for thermoelectric effects studies.[55] We used thiol-terminated (–SH bond) benzene units and found a positive thermopower that increased with increasing molecular length. This is due to the fact that the thermopower increases linearly with length of the molecule, and ultimately increases thermopower. We also observed that in meta configuration, thermopower is more than para configuration due to quantum interference effects.[3]

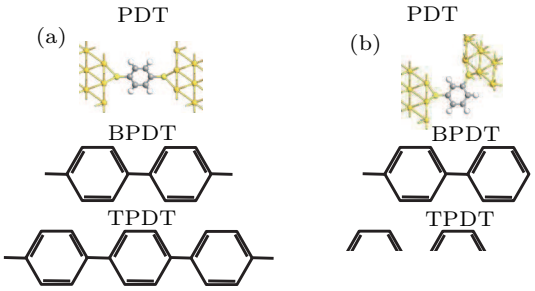


Fig. 1. (color online) Three representative molecules, PDT, BPDT, and TPDT. (a) Para, and (b) meta configurations. Each molecule is coupled to the hollow position of the tips of two gold (111) pyramids via a sulfur atom.

We organize the paper as follows: in Section 2 the model and theoretical formulation are presented. Section 3 presents the main results. The paper ends with conclusions in Section 4.

2. Models and methods

The Hamiltonian of molecule is calculated based on the extended Hückel method and the thermoelectric coefficients are obtained using Green's function method in linear response regime. The system under consideration is composed of an organic molecule which is attached to external electrodes. We developed our own code to perform computational calculations. The physics formulation of the code is based on steps introduced in Zahid.[56] The Hamiltonian of the molecule can be described as follows:

$$H_m = H_{ij} = (C/2)S_{ij}(H_{ii} + H_{jj}), \tag{1}$$

where $C = 1.75$ is Hückel coefficient and the rationale for this expression is that energy should be proportional to the energy of the atomic orbitals. It also should be greater when the overlap of the atomic orbitals is greater. The contribution of these effects to the energy is scaled by parameter C. Hoffmann assigned the value of $C = 1.75$ after a study of the effect of this parameter on the energies of the occupied orbitals of ethane.[57] S_{ij} is overlap integral of the atomic orbitals, and H_{ii} and H_{jj} are ionization energies of the orbitals. For calculating the surface Green's function of a given contact used to evaluate the self-energy from Ref. [58]. Consider a semi-infinite solid whose overall Green's function can be written in the form: $G = (ES - H)^{-1}$, we can simplify the problem by a two dimensional unitary transformation to k space, i.e., Fourier transform the two dimensions parallel to the layers.[59] We are only interested in the surface Green's function $g_s(k)$ which can be shown to satisfy the recursive relation: $g_s(k) = (\alpha(k) - \beta(k)g_s(k)\beta^{\dagger}(k))^{-1}$, this equation can either be solved analytically (if the matrices α and β are one-dimensional) or by iteration starting from a reasonable guess for $g_s(k)$. We can then transform it back to real space by summing over the allowed k vectors (using periodic boundary conditions with N unit cells in each direction). We now express the details of surface Green's function calculation for a gold (111) surface. To find the $\alpha(k) = ES(k) - H(k)$ and $\beta(k)$ we need overlap and Hamiltonian matrices in real space. These were obtained from Hückel Hamiltonian and overlap matrix of a 13-atom gold cluster. $\alpha(k)$ and $\beta(k)$ are matrices with dimension equal to the number of orbitals in the unit cell. For more details refer to Ref. [56].

Transport properties for all methods are calculated using Landauer–Büttiker transmission formula expressed in terms of Green's function:

$$T(\varepsilon) = \mathrm{Tr}\{G^{\mathrm{r}}(\varepsilon)\Gamma_{\mathrm{L}}(\varepsilon)G^{\mathrm{a}}(\varepsilon)\Gamma_{\mathrm{R}}(\varepsilon)\}, \tag{2}$$

where $\Gamma_\alpha = -2\,\mathrm{Im}\Sigma_\alpha$ is given in terms of the lead α self-energy, Σ_α. The retarded Green's function of the molecule coupled to metallic electrodes can be written as follows:

$$G^{\mathrm{r}}(\varepsilon, V_G) = \left\{(\varepsilon + \mathrm{i}0^+)\boldsymbol{I} - H_{\mathrm{m}} - \Sigma_{\mathrm{L}}(\varepsilon) - \Sigma_{\mathrm{R}}(\varepsilon)\right\}^{-1}, \tag{3}$$

where 0^+ is an infinitesimal value. The advanced Green's function can be obtained by relation $G^{\rm a}(\varepsilon) = [G^{\rm r}(\varepsilon)]^{\dagger}$.

Applying a temperature gradient, ΔT can induce a voltage difference ΔV across the system. In the linear response regime in which the temperature gradient and voltage difference are small, the charge current I and heat (energy) current I_Q flowing through the system can be expanded to the first order in terms of ΔT and ΔV:

$$I = {\rm e}^2 L_0 \Delta V + \frac{e}{T} L_1 \Delta T,$$
$$I_Q = -eL_1 \Delta V - \frac{1}{T} L_2 \Delta T \qquad (4)$$

with $L_n = -\hbar^{-1} \int {\rm d}\varepsilon (\varepsilon - \mu)^n T(\varepsilon) (\partial f / \partial \varepsilon)$, where $f(\varepsilon)$ corresponds to equilibrium Fermi–Dirac function and μ is the chemical potential. The temperature T was set to 300 K in our simulations.

Thermoelectric coefficients are expressed in terms of quantities L_n, which can be easily determined when transmission through the molecule system is found. The electric and electron thermal conductances are equal to $G_{\rm e} = {\rm e}^2 L_0$ and $\kappa_{\rm el} = T^{-1}(L_2 - L_1^2/L_0)$, respectively. In the present paper, we consider the linear response case, which indicates that both bias voltage and temperature differences between the two leads tend to zero, i.e., $\mu_{\rm L} = \mu_{\rm R} = \mu$ and $T_{\rm L} = T_{\rm R} = T$. Thermopower is the ratio of induced voltage difference to the applied temperature gradient in the vanishing current, therefore $S = -\Delta V / \Delta T = -(1/eT)(L_1/L_0)$. Finally thermoelectric efficiency of the system is described by a dimensionless parameter, $ZT = S^2 G_e T / \kappa$. The thermal conductance is composed of two parts: $\kappa = \kappa_{\rm el} + \kappa_{\rm ph}$, where $\kappa_{\rm el}$ is electron thermal conductance and $\kappa_{\rm ph}$ denotes phonon thermal conductance which in the case of organic molecular junctions can be ignored due to the existence of a considerable mismatch between density of states of the phonons in metallic electrodes and phonon modes of the molecule that dramatically decreases the phonon transmission.[60,61] Therefore we ignore $\kappa_{\rm ph}$[62] and consider the maximum of ZT. If we consider $\kappa_{\rm ph}$, then there is a small reduction in ZT. In other works, the value of phonon thermal conductance was calculated for para and meta configurations of benzene rings. In this paper, the peaks of minimum and maximum of electrical thermal conductance in meta and para configurations for BPDT molecular junction is about 40 pW/K, and 160 pW/K , respectively. Our results show that electrical thermal conductance is more than phonon thermal conductance in Ref. [63]. Results show that the role of phonons is negligible. We obtain the maximum value of ZT for molecular junction and ignore phonon thermal conductance. On the other hand, experimental results show that thermopower of phenyl derivatives linearly depends on the length of the molecule, that is a sign of ballistic transport in which the effect of phonons can be ignored.[15,32,35]

3. Results and discussion

We begin by considering a simple model for benzene structures, which captures essential physical mechanism responsible for interesting thermoelectric properties of benzene. The schematic structure of a transport junction with benzene molecules sandwiched between two leads is shown in Fig. 1. In order to construct the junctions, each molecule is coupled to the hollow position of the tips of two gold (111) pyramids via a sulfur atom.

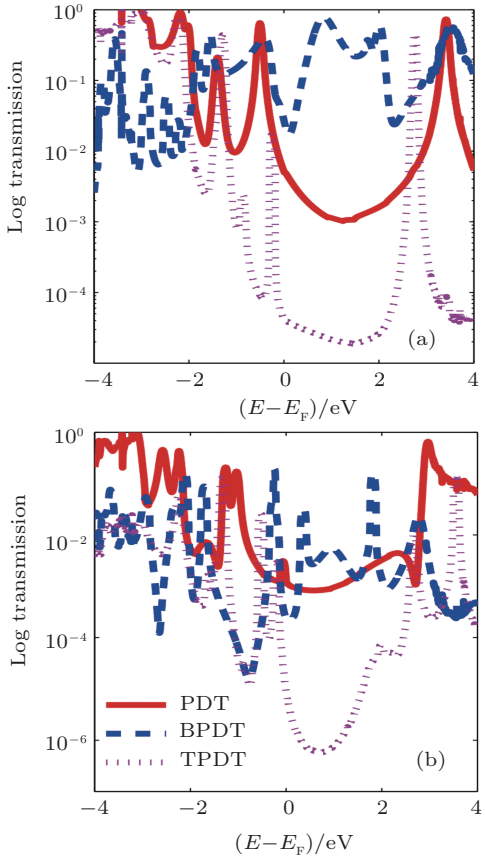


Fig. 2. (color online) Logarithm of transmission coefficient of different geometries of Au/molecule/Au junction versus energy. (a) Para, and (b) meta configurations.

Figure 2 shows the logarithm of transmission coefficient for para and meta configurations, in the case of PDT, BPDT, and TPDT molecular junctions, respectively. Figure 2(b) clearly shows that the transmission coefficient is more different in meta configuration in comparison with para one that results from quantum interference between electronic waves passing through upper and lower branches of molecular rings due to destructive interference between them. It can affect transport properties of the system.[46,47] It is obvious from Fig. 2(b) that most of transmission peaks are mainly changed in height in comparison with Fig. 2(a). The dramatic reduction of transmission coefficient at the Fermi energy ($E_{\rm F}$) in meta configuration can be interpreted as a form of destructive quantum interference.[3]

Figures 3 and 4 show the electrical and electron thermal conductances as a function of the chemical potential of elec-

trodes for different coupling geometries. The electrical and electron thermal conductances have similar behavior for considered configurations. The change in height of peaks in meta coupling with respect to para is due to interferometric nature of molecular system. Figures 3(a) and 3(b) show that the maximum of electrical conductance in para and meta configurations are highest for BPDT molecular junction in some chemical potentials. The value of electrical conductance increases in BPDT molecular junction compared with PDT. This is due to the fact that energy levels of π-electrons get closer to each other by increasing molecular length in para and meta configurations. In TPDT molecular junction compared with BPDT, the value of electrical conductance decreases. This is because of the reduction of transmission coefficient in Fermi energy. This behavior is clearly shown in the inset to Figs. 3(a) and 3(b). Figure 3(b) shows that the maximum of electrical conductance in meta configuration is highest for PDT molecular junction, in negative chemical potentials. The value of electrical conductance in BPDT and TPDT molecular junctions decreases in comparison to PDT, which is because of the rearrangement in energy levels of π-electrons and reduction of transmission coefficient in Fermi energy.

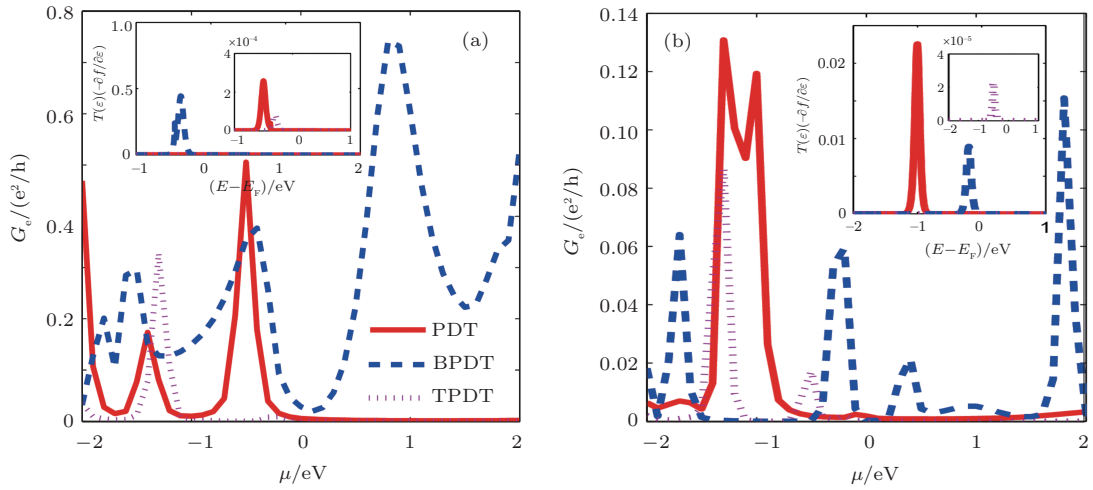


Fig. 3. (color online) The effect of coupling geometry on electrical conductance of Au/(PDT/BPDT/TPDT)/Au junction versus chemical potential of electrodes. (a) Para, and (b) meta configurations; $T = 300$ K. The inset to panels (a) and (b) denotes the quantity $T(\varepsilon)(-\partial f/\partial\varepsilon)$. The inner inset shows hidden curves of outer inset with more resolution.

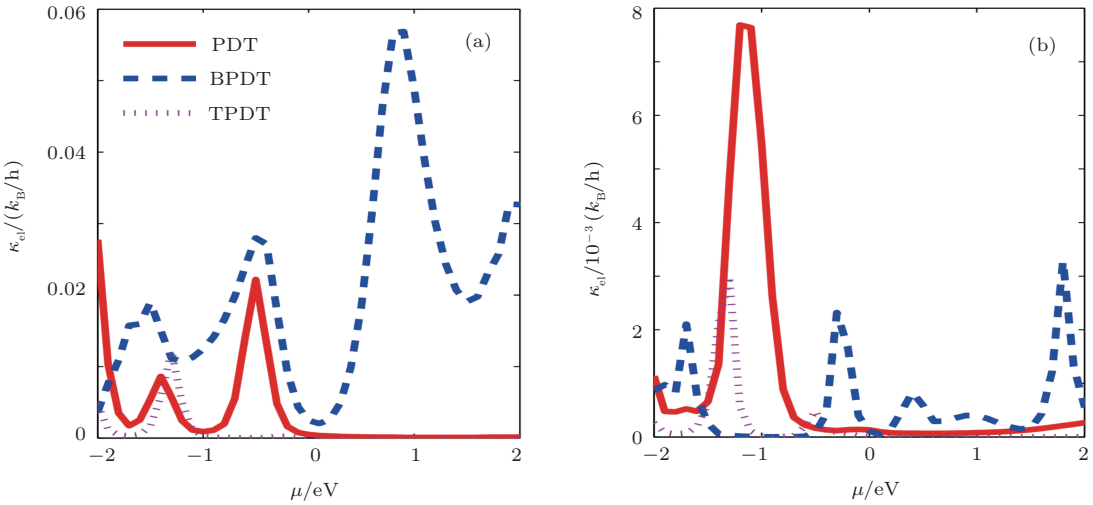


Fig. 4. (color online) The effect of coupling geometry on electron thermal conductance of Au/(PDT/BPDT/TPDT)/Au junction versus chemical potential of electrodes. (a) Para, and (b) meta configurations; $T = 300$ K.

Figures 4(a) and 4(b) show that the maximum of electron thermal conductance in para and meta configurations are highest for BPDT molecular junction in some chemical potentials. The value of electron thermal conductance increases by increasing molecular length in BPDT molecular junction compared with PDT, because electrons and holes transfer more energy in para and meta configurations. But in the case of TPDT molecular junction compared with BPDT, the value of electron thermal conductance is reduced by increasing the molecular length in para and meta configurations. In this case, the transmission coefficient peak moves farther to Fermi derivative and thermopower decreases (Fig. 3(a)).

The value of electron thermal conductance for all molecules, decreases by increasing the molecular length in meta con-

figuration in negative chemical potentials because the overlap of transmission coefficient and Fermi derivative decreases by increasing molecular length (Fig. 3(b)). There is also a reduction of transmission coefficient in Fermi energy because of rearrangement in the energy levels of π-electrons.

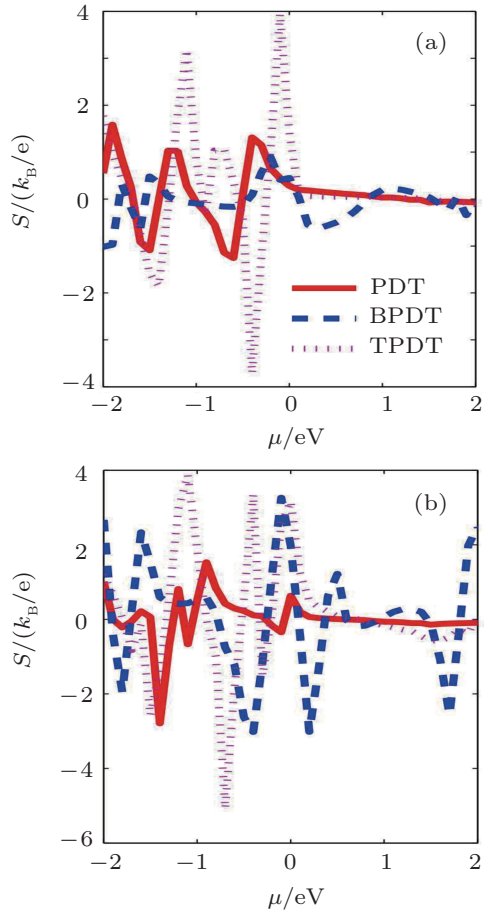


Fig. 5. (color online) The effect of coupling geometry on thermopower of Au/(PDT/BPDT/TPDT)/Au junction versus chemical potential of electrodes. (a) Para, and (b) meta configurations; $T = 300$ K.

Figure 5 shows thermopower of para and meta couplings as a function of the chemical potential of electrodes. We find that thermopower develops sawtooth and oscillatory behaviors due to electronic excitation and change of the electron population in molecule.[64–66] The change in thermopower in terms of gate voltage is clarified by the change in Fermi level of the electrodes due to the applying gate voltage. The change in Fermi level can alter electrons population inside the molecule. This alteration in electrons population leads to sawtooth and oscillatory behaviors in thermopower. The change in chemical potential of electrodes changes the distance between molecular energy levels and Fermi energy, therefore the dominant carriers in transport change, and electrons or holes flowing from left to the right electrode. The location of Fermi energy level can also be found from the sign of thermopower: negative (positive) sign denotes the location close to LUMO (HOMO).[35]

Different binding positions can lead to substantial variations of thermopower mostly due to the changes in alignment of the frontier molecular orbital levels and the Fermi energy.[32] It has been suggested that the sign of thermopower provides information of whether transport is mainly via occupied or unoccupied molecular states[26] The sign of thermopower changes in the vicinity of electron–hole symmetry points and resonance energies, in which S is zero in these points. Both carriers in transport mechanism, have equal contribution but with opposite sign (the net-induced voltage drop is zero) in symmetry points. The temperature gradient cannot produce a net electrical current (the induced voltage drop is zero) because electrons can tunnel from colder and hotter electrodes to molecular levels without needing thermal energy in resonance energies. The important factor for figure of merit is thermopower. The figure of merit tends to zero when thermopower tends to zero.

Figure 5(a) shows that thermopower increases by increasing molecular length because of rearrangement in energy levels which are getting closer in para configuration. But in BPDT molecular junction, thermopower will decrease, because the difference between Fermi energy and peak of transmission coefficient is decreased. Figure 5(b) shows that thermopower increases by increasing molecular length in meta configuration because of the reduction of HOMO–LUMO gap.

The value and number of oscillations for some energy increase by molecular length in both configurations. This is because of the increasing number of π-electrons due to the enhancement of molecular length which increases the number of electrons tunneling through molecular energy levels. Our calculations show that the figure of merit strongly depends on molecular length and molecular junction geometry so that ZT increases by increasing molecular length in meta configuration (see Fig. 6(b)). This is due to the fact that thermopower increases linearly by length of the molecule and figure of merit is directly related to the square of thermopower (see Figs. 5 and 6) in meta configuration.

Figure 6(a) shows that the value of the ZT increases in TPDT molecular junction compared with BPDT, because TPDT molecular junction has smaller κ_{el} and larger S, and thus, a larger ZT compared with BPDT molecular junction in para configuration. But ZT decreases by increasing molecular length in para configuration in PDT molecular junction compared with BPDT because BPDT molecular junction has larger κ_{el} and smaller S, and thus, a smaller ZT compared with PDT molecular junction in para configuration. ZT increases when electrical conductance and thermopower are maximum, because the change in ZT is based on Fermi energy. Therefore when the Fermi energy is close to energy levels of molecule,

the resonant occurs and electrical conductance increases. ZT increases dramatically by increasing electrical conductance and thermopower in some Fermi energies. This enhancement is more in meta configuration, because the value of thermopower in meta configuration is more than para configuration due to quantum interference effects and meta configuration has smaller κ_{el} and thus, a larger ZT. The figure of merit is directly related to the square of thermopower, and the value of ZT is more sensitive to S. Therefore the main factor for figure of merit is thermopower. Note that the maximum of ZT can only be found in some specific geometries. In fact, our calculations predict that the change of coupling geometry and molecular length can alter the thermoelectric efficiency.

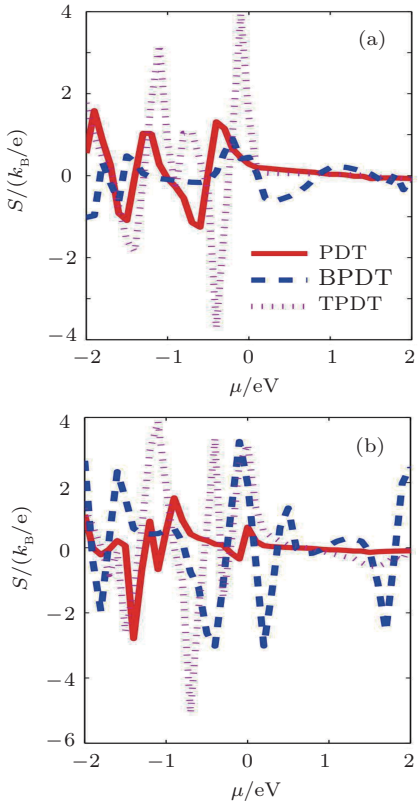


Fig. 6. (color online) The effect of coupling geometry on the figure of merit of Au/(PDT/BPDT/TPDT)/Au junction versus chemical potential of electrodes. (a) Para, and (b) meta configurations; $T = 300$ K.

The increase of thermopower with number of rings (N), in Fermi energy ($E - E_F = 0$ eV) as indicated by measurements, is well reproduced by our computational results and is also consistent with recent computational studies.[15,32,35] The increase of thermopower by increasing molecular length in meta configuration is more than para configuration, see Fig. 7. This is solely due to the effect of quantum interference that anchoring is placed too close to the position of molecule where interference effects occur.[3] Since the Fermi energy lies closer to HOMO level than to LUMO level, see Fig. 2, thermopower in the Fermi energy ($E - E_F = 0$ eV), see Fig. 2, has a positive value therefore transport is p-type. Thermopower is maximum when peak of transmission coefficient is close to the Fermi energy and overlapping between transmission coefficient and Fermi derivative is more in the vicinity of the Fermi energy, see Fig. 7. We also find that thermopower increases roughly linearly with N, as suggested by experiments.[32] The slope of transmission function at E_F is negative for all thiol-terminated junctions in Fig. 2. Thermopower increases by increasing molecular length in both configurations. The magnitude of slop changes in meta configuration is more than para configuration by increasing molecular length.

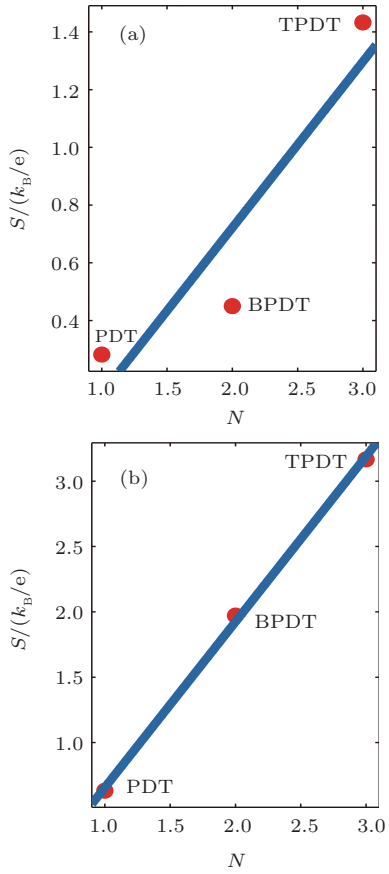


Fig. 7. (color online) The effect of coupling geometry on the thermopower of Au/molecule/Au junction versus number of aromatic rings in (a) para, and (b) meta configurations. The magnitude of slop is 0.58 for para, and 1.27 for meta configuration; $T = 300$ K.

Figure 8 shows the figure of merit versus the number of aromatic rings (N), in Fermi energy $E - E_F = 0$ eV in para and meta couplings. The increase of figure of merit by increasing molecular length in meta configuration is more than para configuration. ZT increases by increasing electrical conductance and thermopower in Fermi energy $E - E_F = 0$ eV. This increase is more in meta configuration in Fermi energy $E - E_F = 0$ eV, because the value of S in meta configuration is more than para configuration due to interference effects. The figure of merit increases roughly linearly with N, in Fermi energy $E - E_F = 0$ eV in para and meta configurations. We also find that the magnitude of slop changes in meta configuration is more than para configuration by increasing molecular length, in Fermi energy $E - E_F = 0$ eV.

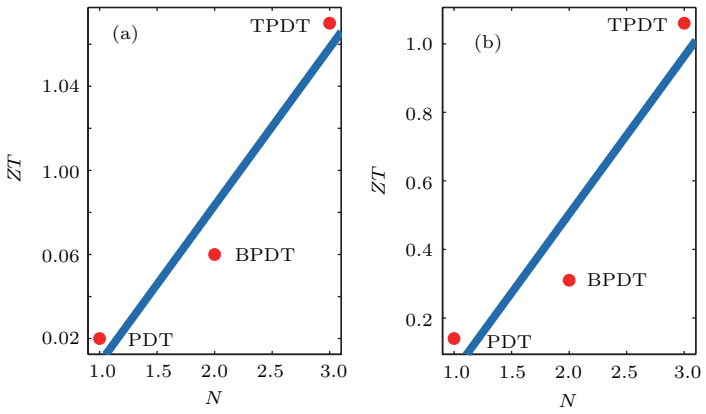


Fig. 8. (color online) The effect of coupling geometry on the figure of merit of Au/molecule/Au junction versus number of aromatic rings in (a) para, and (b) meta configurations. The magnitude of slop is 0.07 for para, and 0.46 for meta configuration; $T = 300$ K.

4. Conclusion

We studied thermoelectric properties of three organic molecules attached to three-dimensional gold electrodes in two different configurations (para and meta) with thiol-terminated junctions, using Green's function method in linear response regime. In conclusion, we analyzed length-dependence properties of conductance and thermopower for contacts. Our studies indicate that thermopower of thiol-terminated junctions is positive in sign and increases with the length of molecule. We observe that thermopower and figure of merit increase linearly with length of the molecule. Molecular transport properties are highly sensitive to molecule-to-lead interface geometry. Thermopower in meta configuration is more than para configuration due to quantum interference effects. With increasing molecular length, slope changes in meta configuration is more. We also express that interference effects and increasing molecular length can increase the thermoelectric efficiency of device in a specific configuration. In the present study, the effects of electron-electron correlation is ignored and calculations are performed in the absence of dephasing process. Incorporating all these effects have been left for future studies and warrants a more detailed investigation.

References

[1] Vazquez H, Skouta R, Schneebeli S, Kamenetska M, Breslow R, Venkataraman L and Hybertsen M S 2012 *Nat. Nanotechnol.* **7** 663
[2] Guédon C M, Valkenier H, Markussen T, Thygesen K S, Hummelen J C and Molen S J 2012 *Nat. Nanotechnol.* **7** 305
[3] Arroyo C R, Tarkuc S, Frisenda R, Seldenthuis J S, Woerde C H, Eelkema R, Grozema F C and Zant H S 2013 *Angew. Chem. Int. Ed.* **52** 3152
[4] Ballmann S, Härtle R, Coto P B, Elbing M, Mayor M, Bryce M R, Thoss M and Weber H B 2012 *Phys. Rev. Lett.* **109** 056801
[5] Solomon G C, Andrews D Q, Hansen T, Goldsmith R H, Wasielewski M R, Van Duyne R P and Ratner M A 2008 *J. Chem. Phys.* **129** 054701
[6] Solomon G C, Andrews D Q, Goldsmith R H, Hansen T, Wasielewski M R, Van Duyne R P and Ratner M A 2008 *J. Am. Chem. Soc.* **130** 17301
[7] Solomon G C, Bergfield J P, Stafford C A and Ratner M A 2011 *Beilstein J. Nanotechnol.* **2** 862
[8] Härtle R, Butzin M, Rubio-Pons O and Thoss M 2011 *Phys. Rev. Lett.* **107** 046802
[9] Bergfield J P, Solomon G C, Stafford C A and Ratner M A 2011 *Nano Lett.* **11** 2759
[10] Markussen T, Stadler R and Thygesen K S 2010 *Nano Lett.* **10** 4260
[11] Markussen T, Stadler R and Thygesen K S 2011 *Phys. Chem. Chem. Phys.* **13** 14311
[12] Markussen T and Thygesen K S 2014 *Phys. Rev. B* **89** 085420
[13] Ashcroft N W and Mermin N D 1976 *Solid State Physics* (New York: Holt, Rinehart and Winston)
[14] Majumdar A 2004 *Science* **303** 777
[15] Ke S H, Yang W, Curtarolo S and Baranger H U 2009 *Nano Lett.* **9** 1011
[16] Venkatasubramanian R, Siivola E, Colpitts T and O'quinn B 2001 *Nature* **413** 597
[17] Harman T C, Taylor P J, Walsh M P and LaForge B E 2002 *Science* **297** 2229
[18] Hsu K F, Loo S, Guo F, Chen W, Dyck J S, Uher C, Hogan T, Polychroniadis E K and Kanatzidis M G 2004 *Science* **303** 818
[19] Jiang J W, Wang J S and Li B 2010 *J. Appl. Phys.* **109** 014326
[20] Markussen T, Jauho A P and Brandbyge M 2009 *Phys. Rev. B* **79** 035415
[21] Xie Z X, Tang L M, Pan C N, Li K M, Chen K Q and Duan W 2012 *Appl. Phys. Lett.* **100** 073105
[22] Pan C N, Xie Z X, Tang L M and Chen K Q 2012 *Appl. Phys. Lett.* **101** 103115
[23] Zhou Y, Dong J and Li H 2015 *RSC Adv.* **5** 66852
[24] Dong J, Li H and Li L 2013 *NPG Asia Mater.* **5** e56
[25] Markussen T, Jauho A P and Brandbyge M 2008 *Nano Lett.* **8** 3771
[26] Paulsson M and Datta S 2003 *Phys. Rev. B* **67** 241403
[27] Koch J, Oppen F, Oreg Y and Sela E 2004 *Phys. Rev. B* **70** 195107
[28] Segal D 2005 *Phys. Rev. B* **72** 165426
[29] Reddy P, Jang S Y, Segalman R A and Majumdar A 2007 *Science* **315** 1568
[30] Baheti K, Malen J A, Doak P, Reddy P, Jang S Y, Tilley T D, Majumdar A and Segalman R A 2008 *Nano Lett.* **8** 715
[31] Kubala B, König J and Pekola J 2008 *Phys. Rev. Lett.* **100** 066801
[32] Pauly F, Viljas J K and Cuevas J C 2008 *Phys. Rev. B* **78** 035315
[33] Murphy P, Mukerjee S and Moore J 2008 *Phys. Rev. B* **78** 161406
[34] Finch C M, Garcia-Suarez V M and Lambert C J 2009 *Phys. Rev. B* **79** 033405
[35] Aradhya S V and Venkataraman L 2013 *Nat. Nanotechnol.* **8** 399
[36] Liu Y S and Chen Y C 2009 *Phys. Rev. B* **79** 193101
[37] Liu Y S, Yao H T and Chen Y C 2011 *J. Phys. Chem. C* **115** 14988
[38] Quek S Y, Choi H J, Louie S G and Neaton J B 2010 *ACS Nano* **5** 551
[39] Balachandran J, Reddy P, Dunietz B D and Gavini V 2012 *J. Phys. Chem. Lett.* **3** 1962
[40] Karlström O, Strange M and Solomon G C 2014 *J. Chem. Phys.* **140** 044315
[41] Ke S H, Yang W, Curtarolo S and Baranger H U 2009 *Nano Lett.* **9** 1011
[42] Zotti L A, Bürkle M, Pauly F, Lee W, Kim K, Jeong W, Asai Y, Reddy P and Cuevas J C 2014 *New J. Phys.* **16** 015004

[43] Bürkle M, Hellmuth T J, Pauly F and Asai Y 2015 *Phys. Rev. B* **91** 165419
[44] Strange M, Seldenthuis J S, Verzijl C J O, Thijssen J M and Solomon G C 2015 *J. Chem. Phys.* **142** 084703
[45] Golsanamlou Z, Tagani M B and Soleimani H R 2015 *Commun. Theor. Phys.* **64** 361
[46] Dey M, Maiti S K and Karmakar S N 2011 *Org. Electron.* **12** 1017
[47] Dutta P, Maiti S K and Karmakar S N 2010 *Org. Electron.* **11** 1120
[48] Chen F, Li X, Hihath J, Huang Z and Tao N 2006 *J. Am. Chem. Soc.* **128** 15874
[49] Peng G, Strange M, Thygesen K S and Mavrikakis M 2009 *J. Phys. Chem. C* **113** 20967
[50] Moreno-García P, Gulcur M, Manrique D Z, Pope T, Hong W, Kaliginedi V, Huang C, Batsanov A S, Bryce M R, Lambert C and Wandlowski T 2013 *J. Am. Chem. Soc.* **135** 12228
[51] Bürkle M, Zotti L A, Viljas J K, Vonlanthen D, Mishchenko A, Wandlowski T, Mayor M, Schön G and Pauly F 2012 *Phys. Rev. B* **86** 115304
[52] Dubi Y 2013 *New J. Phys.* **15** 105004
[53] Dubi Y 2013 *J. Chem. Phys.* **138** 114706
[54] Ludoph B and Van Ruitenbeek J M 1999 *Phys. Rev. B* **59** 12290
[55] Ramezani Akbarabadi S, Golsanamlou Z and Rahimpour Soleimani H 2014 *Curr. Phys. Chem.* **4** 285
[56] Zahid F, Paulsson M and Datta S 2003 "Electrical conduction through molecules", *Advanced Semiconductors and Organic Nano-Techniques* **3**
[57] Ramachandran K I, Deepa G and Namboori K 2008 *Springer Science and Business Media*
[58] Samanta M 1995 Purdue University
[59] redAshcroft N W and Mermin N D 1976 *Solid State Physics* (Philadelphia: Saunders College Publishing)
[60] Rego L G and Kirczenow G 1999 *Phys. Rev. B* **59** 13080
[61] Wang R Y, Segalman R A and Majumdar A 2006 *Appl. Phys. Lett.* **89** 173113
[62] Golsanamlou Z, Tagani M B and Soleimani H R 2015 *Phys. Chem. Chem. Phys.* **17** 13466
[63] Klöckner J 2014 *Phonon Transport and Thermoelectric Properties of Molecular Contacts* (University of Konstanz)
[64] Tagani M B and Soleimani H R 2013 *J. Appl. Phys.* **113** 143709
[65] Tagani M B and Soleimani H R 2012 *Solid State Commun.* **152** 914
[66] Golsanamlou Z, Tagani M B and Soleimani H R 2014 *Macromolecular Theory and Simulations* **23** 311